

# Tandem mass spectrometry approaches for recognition of isomeric compounds mixtures

Sara Crotti<sup>1</sup> | Marta Menicatti<sup>2</sup> | Marco Pallecchi<sup>2</sup> | Gianluca Bartolucci<sup>2</sup>

<sup>1</sup>Fondazione Istituto di Ricerca Pediatrica  
Città della Speranza, Padova, Italy

<sup>2</sup>Dipartimento Neurofarba, Università di  
Firenze, Florence, Italy

## Correspondence

Gianluca Bartolucci, Dipartimento  
Neurofarba, Università di Firenze, via U.  
Schiff 6, 50019 Sesto Fiorentino, Firenze,  
Italy.

Email: [gianluca.bartolucci@unifi.it](mailto:gianluca.bartolucci@unifi.it)

## Abstract

The present review aims to collect the published literature pertaining the recognition of isobaric compounds (isomers or stereoisomers) using the features of tandem mass spectrometry (MS) experiments without any chromatographic separation or chemical modification (derivatization or isotopic enrichment) of the analytes. MS/MS methods possess high selectivity, wide dynamic range and high throughput capabilities. Generally, tandem MS has limited capability for distinguishing isomers that fragment similarly. However, some MS/MS methods have been developed and positively applied to isomers discrimination. Among the literature on this topic, the applications that fit on the review subject can be summarized as follow: (1) chiral discrimination by the kinetic method, (2) the use energy-resolved tandem mass spectra and the survival yield (SY) representation, (3) the kinetics evaluation of the ion-molecule interaction and (4) the postprocessing mathematical algorithm to resolve the isomers in MS/MS signal.

## KEYWORDS

ion-molecule interaction, isomers, kinetic method, LEDA, MS/MS, survival yield

## 1 | INTRODUCTION

Mass spectrometry (MS) is an analytical technique largely employed to obtain information not only on the molecular weight of the analytes but also on their structure, by the analysis of the fragment ions. However, the specificity of MS signal may be compromised when the compounds show both common precursor ions and similar chromatographic retention properties, as in the case of isomers analysis. Frequently, similar MS/MS

product ions are generated, creating difficulties if the isomers under analysis are present at unknown concentrations. Despite these aspects, the interest in MS for isomers characterization is largely increased, due to the important role of molecular asymmetry in biological systems. Indeed, biologically relevant responses of active compounds such as drugs, endogenous mediators, or xenobiotics rely upon receptor affinity to a specific isomer, whilst other isomers may be inactive or toxic. Then, the application of MS to the isomers analysis has evolved

**Abbreviations:** CCV, characteristic collision voltage; CID, collision induced dissociation; ECD, electron capture dissociation; ee, enantiomeric excess; ERMS, energy resolved mass spectrometry; ESI, electrospray ionization; ETD, electron transfer dissociation; FIA, flow injection analysis; GPCP, gas-phase collisional purification; IM, ion mobility; IM-MS, ion mobility-mass spectrometry; LC-MS, liquid chromatography-mass spectrometry; LEDA, linear equations deconvolution analysis; MRM, multiple-reaction monitoring; MS<sup>n</sup>, sequential MS/MS experiments; MS/MS, tandem mass spectrometry; PTM, posttranslational modification; SY, survival yield.

This is an open access article under the terms of the Creative Commons Attribution-NonCommercial-NoDerivs License, which permits use and distribution in any medium, provided the original work is properly cited, the use is non-commercial and no modifications or adaptations are made.

© 2021 The Authors. *Mass Spectrometry Reviews* published by John Wiley & Sons Ltd.

by exploring different approaches, which include collisional experiments, analytes derivatization/interaction with isomers, or chromatographic/ion mobility (IM) separation (Awad & El-Aneel, 2013).

In the simplest scenario, when similarly fragmenting isomers are present in a mixture, it is common practice to try to separate them chromatographically. However, this approach may require the set-up of ad hoc sample preparation procedures and the evaluation of different chromatographic columns to obtain adequate analytes separation. All these procedures are usually molecule-specific and rarely can be extended to other compounds. Moreover, in the case of isomers having different thermodynamical stability, sample racemization during preparative procedures may occur, as in the case of photo-isomerization of Z-Sunitinib in solution (Posocco et al., 2018). Some attempts to resolve isomers by using single-stage MS have been performed by reacting an isomer (Host) with a mixture of isotopically labeled/unlabeled enantiomers (Guest) to form complexes with detectable mass difference (Sawada et al., 1998). Despite the simplicity of this approach, quantitative analyzes of isomers mixtures cannot be performed. Recently, through the introduction of IM instruments, the isomers resolution become possible thanks of the influence of molecular shape on drift times (Lapthorn et al., 2013). The application of IM-MS in isomers analysis is useful, being possible to analyze both small compounds and large biomolecules (Wu et al., 2020). Typical IM applications, explored the opportunity to separate isomeric carbohydrates (Clowers et al., 2005), lipids (Chouinard et al., 2017), or peptide isomers (Creese et al., 2013). However, this technique requires dedicated and expensive instrumental systems, not available in most of laboratories, thus its potentiality are far to be routinely applied.

MS/MS methods are attractive for many applications owing to their high selectivity, wide dynamic range and high throughput capabilities. Generally, MS/MS shows poor specificity in isomers distinction. Some authors explored the possibility to resolve isomers by MS/MS on the basis of “diagnostic fragments” intensity. The use of diagnostic fragment ions ratio to resolve isomers has been applied for those compounds having fragmentation routes that differ sufficiently, so that parent ions lead to different fragment ions. This approach has been applied for the separation and identification of polymeric macrocycles in which the MS/MS is suitable for the differentiation of linear and cyclic architectures whose molecular ions exhibit distinct fragmentation characteristics. Conversely, deeper investigations regarding differences in macromolecular sizes and shapes have been evaluated using IM-MS (Yol & Wesdemiotis, 2014). Generally, isomers show the same product ions and, even if different branching ratio are present, it is hardly to

distinguish them without the support of chromatographic separations. Consequently, very few cases report a clear difference between MS/MS spectra of isomers, which limits this approach in the isomers mixtures analysis (Nunez et al., 2018).

MS/MS methods have been used to recognize the post-translational modification (PTM) of proteins, such as acetylation or amino-acid isomerization. Proteins acetylation is one of the major PTM in eukaryotes and the interplay between acetylation and deacetylation is crucial for many cellular processes (Drazic et al., 2016). In the typical case of a protein having two possible acetylation sites, each acetylated form represents an isomer and MS alone would not be informative. However, if ionization efficiency is the same, MS/MS fragment ions differentiate the two positional isomers and provide data on the relative amount of acetylation on each residue (Pesavento et al., 2006). Similarly, amino-acid isomerization (as in the case of Asp/isoAsp) is a hallmark of protein aging and may be implied in the age-related pathological states, like Alzheimer's disease (Lambeth et al., 2019). Also for biological drugs, the substitution of  $\beta$ -amino acids by  $\alpha$ -amino acids has been introduced to increase their in vivo activity and stability (Cabrele et al., 2014). The discrimination between aspartate and isoaspartate (Asp and isoAsp) containing peptides can be highlighted by low-energy CID (Lehmann et al., 2000). Through the observation that the intensity of *b*- and *y*-fragment ions generated by the cleavage adjacent to the Asp/isoAsp site and the intensity immonium ion at *m/z* 88 are related to the isomer present, it is possible to identify the right amino acid. Indeed, when Asp is replaced by isoAsp in the peptide sequence, the *b/y* intensity ratio of complementary *b*- and *y*-ions (from the C- and the N-terminal sites) is generally decreased, and the same occurs for the immonium ion abundance. An analogous approach has been developed more recently, using the  $[M + Na]^+$  ions from Asp/isoAsp-containing peptides (Wang et al., 2011).

In absence of evident differences in MS/MS spectra, alternative approaches can be employed. For instance, the investigation of MS<sup>3</sup> mass spectra or the selection of different ion species as precursor ions (e.g., cationized species with alkali metal ions) can positively lead to characterization of the isomers (Basso et al., 2003; Ramesh et al., 2011). These approaches represent a fast and valid alternative for structural isomers characterization. For both, isomers have been discriminated by a direct infusion into the ESI source, avoiding any chromatographic separation.

Of note, beside low-energy CID, which induces reduced ion fragmentation via low energy collisions, the ion fragmentation performed at higher collision energies

is another possible approach for isomer characterization (Pittenauer & Allmaier, 2009). By the high-energy CID, the excess energy goes on to secondary fragmentation pathways, providing increased structural information and isomer-specific MS/MS spectra (Scrivens et al., 2003; Subramaniam et al., 2011). Other dissociation methods, such as electron capture and transfer dissociations (ECD and ETD), are widely used to induce secondary fragmentation of biomolecules. By these approaches, amino acids side chain fragments and isomer can be differentiated. Both ECD and ETD have a great impact in proteomics, where amino-acids isomerization is usually very difficult to analytically differentiate using MS (Hurtado & O'Connor, 2012).

Most of above discussed MS/MS approaches are hardly generalizable because of they rely on compound-specific solutions. Instead, the present review aims to describe those tandem MS strategies capable to characterize and quantify isomers and/or isobars in mixtures via a standardizable approach, applicable to different compounds. The challenge is to achieve an adequate specificity to distinguish the isomers present in the sample without the support of any structural manipulation (i.e., derivatization and/or isotopic enrichment) or chromatographic separation. The use of right approach provides many analytical advantages, among which the most important are the sensitivity, the reliability and the faster analysis.

Therefore, the aspects of the MS/MS methods that might be permit to discriminate between the isomers are evaluated. Concerning this, fundamental steps to consider are the selection of precursor ion, its fragmentation through CID mechanism and the product ions analysis. Among the literature on this topic, the applications that fit the above-cited aspects are: (1) the chiral discrimination by the kinetic method, (2) the use energy-resolved tandem mass spectra and the survival yield (SY) representation, (3) the kinetics evaluation of the ion-molecule interaction, and (4) the postprocessing mathematical algorithm to resolve the isomers in MS/MS signal.

## 2 | CHIRAL DISCRIMINATION BY THE KINETIC METHOD

Kinetic method was widely used for the determination of thermochemical properties based on the rates of competitive dissociation of mass-selected cluster ions. Chiral discrimination by the kinetic method is based on the competitive MS/MS dissociation of metal ion-bound cluster ions of R- and S-enantiomers. In this method, the hypothetical three-point interaction, between the

chiral compound and a chiral selector and/or mediator that facilitate chiral recognition, is applied. The rationale for the three-point rule is that it is possible to discriminate between the enantiomers if there are at least three point of interaction between the chiral selector/mediator and one or both of the enantiomers (Berthod, 2010). In gas-phase (i.e., into the ESI source) the interaction between a chiral analyte and a chirally pure substrate, give rise to the creation of diastereomeric complexes having different chemical-physical properties. The competitive dissociation of these complexes, ultimately reflects into relatively large differences in fragment ion-branching ratios (Cooks & Wong, 1998; Cooks et al., 1994).

This approach of chiral analysis experiments was initially applied to ion trapping devices (quadrupole or high capacity ion traps); afterward the triple quadrupole (QqQ) or the hybrid quadrupole-time of flight (Q-ToF) mass spectrometer systems is shown to provide an alternative (Sawada et al., 1998; Wu & Cooks, 2005). Tao, Gozzo, et al. (2001) demonstrated that kinetic method allows quantitative measurements of optical purity. By means of a chiral reference compound (ref\*), chiral analytes ( $A_R$  or  $A_S$ ) are complexed with a transition-metal ion (M) to generate a trimeric complex (Figure 1). The cluster ions so formed  $[M^{II}(A_R \text{ or } S)(\text{ref}^*)_2-H]^+$  have three chiral ligands in one complex comprising 1 molecule of the analyte and 2 molecules of the ref\*. They are single charged by selective ref\* deprotonation and, by means of MS/MS experiments the competitive ligand loss give rise to two possible dissociations:  $[M^{II}(A_R \text{ or } S)(\text{ref}^*)_2-H]^+$

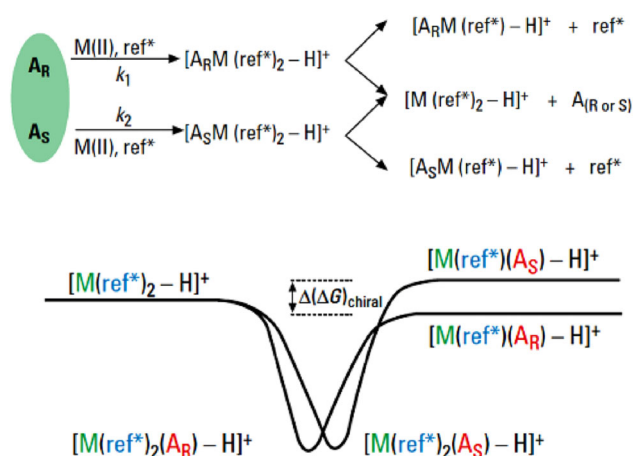


**FIGURE 1** Competitive dissociation of metal ion-bound complexes (above).  $A_R$  or  $A_S$ , chiral analytes; ref\*, chiral reference compound; M(II), transition-metal ion such as Cu(II), Zn(II), or Ni (II). Free-energy diagram for competitive dissociations of metal ion-bound cluster ions of two deprotonated trimeric cluster ions that differ in the chirality of one ligand (Bottom). Reproduced with permission from Tao and Cooks (2003) [Color figure can be viewed at [wileyonlinelibrary.com](http://wileyonlinelibrary.com)]

or  $[M^{II}(\text{ref}^*)_2\text{-H}]^+$ . Generally, in these studies, the gas-phase  $M(\text{II})$  complexes are generated by electrospraying 50/50 water/methanol solutions containing a mixture of the analyte and the reference compound (an R-amino acid), at a concentration of 100  $\mu\text{M}$  each, and 25  $\mu\text{M}$  of a  $M(\text{II})$  salt.

Of note, the MS spectra from the  $M(\text{II})$ , A, and  $\text{ref}^*$  mixtures are constituted by a very complex series of signals, in which different A:  $\text{ref}^*$  stoichiometry may be present at once. This plethora of possible combinations, may potentially affect the method sensitivity because of most of analytes or  $\text{ref}^*$  are potentially involved into useless complexes. Indeed, only the signal arising from the trimeric complexes having 1:2 stoichiometry are useful to evaluate the (R, S) enantiomers. As an example, in Figure 2 it is reported the MS spectrum of the mixture used for the chiral recognition of tartaric acid.

Only the signal at  $m/z$  621 is selected to analyze the tartaric acid enantiomeric composition through the application of tandem MS experiment. The obtained dissociation of trimeric precursor ion leads to the dimeric ions:  $[\text{Ni}(\text{A}_{\text{R or S}})(\text{ref}^*)\text{-H}]^+$  and  $[\text{Ni}(\text{ref}^*)_2\text{-H}]^+$  having different intensities by competitive losses of  $\text{A}_{\text{R or S}}$  or  $\text{ref}^*$ .

Kinetic method has been applied to quantify the enantiomeric excess (*ee*) of amino acids, sugars, peptides and several drugs by the Cooks' group (Augusti, Augusti, et al., 2002; Augusti, Carazza, et al., 2002; Tao & Cooks, 2001; Tao, Gozzo, et al., 2001; Tao, Wu, et al., 2001; Zhang et al., 2001) and by several other authors (Augusti & Augusti, 2005; Chen et al., 2002; Huang et al., 2020; Karthikraj et al., 2014; Kumari et al., 2008; Lee et al., 2008; Ming et al., 2005; Wu et al., 2013), thus confirming the method validity. For instance, Figure 3 reproduce the CID spectra leading to the chiral recognitions of drug ephedrine (Tao, Gozzo, et al., 2001). MS/MS spectra of the complex ion

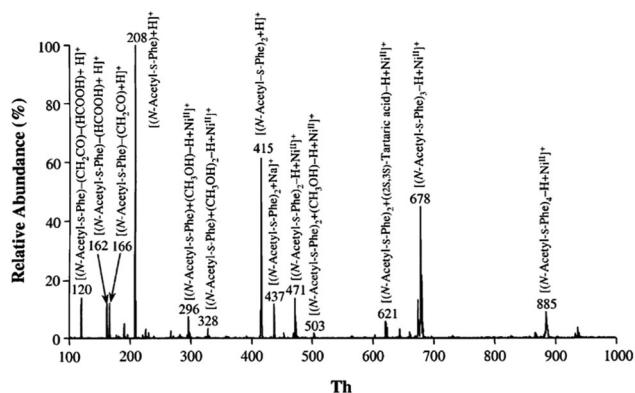


**FIGURE 2** ESI mass spectrum of a sample containing tartaric acid, N-acetyl-s-phenylalanine, and  $\text{NiCl}_2$  in methanol-water solution. Major cluster ions are reported and identified. Reproduced with permission from Wu et al. (2002). ESI, electrospray ionization

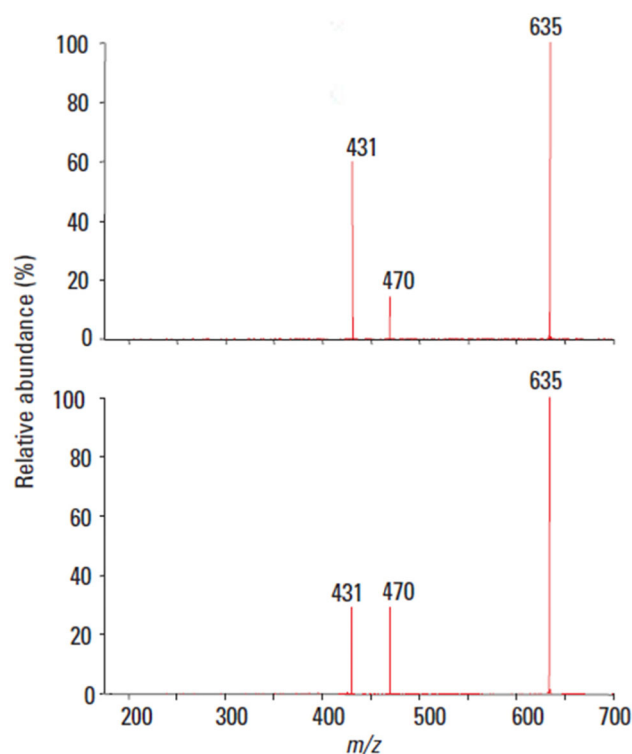


**FIGURE 3**  $\text{MS}^2$  spectrum of  $[\text{Cu}^{II}(\text{L-Trp})_2(\text{ephedrine})\text{-H}]^+$  complex ( $m/z = 635$ ) that contains  $\text{Cu}^{2+}$ , two L-Trp, and (top) (+)-ephedrine or (bottom) (-)-ephedrine. Modified with permission from Tao, Gozzo, et al. (2001) [Color figure can be viewed at [wileyonlinelibrary.com](http://wileyonlinelibrary.com)]

$[\text{Cu}^{II}(\text{ephedrine}_{\text{R or S}})(\text{L-Trp})_2\text{-H}]^+$  at  $m/z = 635$  were obtained and energy differences between the product ions  $[\text{Cu}^{II}(\text{ephedrine}_{\text{R or S}})(\text{L-Trp})\text{-H}]^+$  at  $m/z = 431$  result in differences in their abundances relative to the reference product ion  $[\text{Cu}^{II}(\text{L-Trp})_2\text{-H}]^+$  at  $m/z = 470$ . The two cluster ions, in which ephedrine<sub>R</sub> or ephedrine<sub>S</sub> are involved, yield identical products by one fragmentation route and two diastereomeric product ions with energies that differ by the free-energy change ( $\Delta(\Delta G)_{\text{chiral}}$ ) needed to activate the competitive ligand loss fragmentation (Figure 1). This  $\Delta(\Delta G)_{\text{chiral}}$  is due to differences in steric interactions because of the analytes chirality and influence the degree of chiral discrimination.

As emphasizes in the free-energy diagram for competitive dissociations of metal ion-bound cluster ions (Figure 1, lower panel), parent ions dissociation is a highly endothermic process with a negligible reverse critical energy and it is assumed that the dissociation rate constants are adequately represented by the two fragment ion abundances. Moreover, the more weakly bound precursor complexes show only small differences in energy, giving rise to observed chiral selectivity. Consequently, the ratio between the stabilities (i.e., the intensities) of the product ions ( $[\text{M}(\text{A}_{\text{R}})(\text{ref}^*)\text{-H}]^+$  and



$[M(A_S)(\text{ref}^*)-H]^+$  to the reference complex  $[M(\text{ref}^*)_2-H]^+$  can be calculated (Equation 1).

$$R = \frac{I_R + I_S}{I_{\text{ref}^*}} \quad (1)$$

in which  $I_R$  and  $I_S$  are the intensities signal of  $([M(A_R \text{ or } S)(\text{ref}^*)-H]^+)$  dimeric product ions while  $I_{\text{ref}^*}$  refer to the intensity of the  $[M(\text{ref}^*)_2-H]^+$  ion. The natural logarithm of  $R$  ( $\ln R$ ) can be calculated, and it is linearly related to the enantiomeric purity of the analytes (Tao et al., 2000; Tao, Gozzo, et al., 2001).

The relationship between the  $\ln R$  and the analytes  $ee$  can be extrapolated from the kinetic method (Cooks & Wong, 1998) and the energy difference is proportional to the  $\ln R$ , as follows (Equation 2).

$$\ln R = \frac{\Delta(\Delta G)}{RT_{\text{eff}}} \quad (2)$$

where  $R$  in the denominator is the gas constant,  $T_{\text{eff}}$  is the effective temperature of the activated complex.

Using samples of known  $ee$ , it is possible to construct a calibration curve (Figure 4). To do this, the calibration curves of compound of interest (as an example, proline and phenylalanine in Figure 4) is obtained by plotting the ratio of two fragment ions (single ratio method) to the  $ee$  of pure enantiomers.

If both enantiomers (S, R or D, L) are available as pure compounds, it is possible to calculate the chiral selectivity ( $R_{\text{chiral}}$ ), which is defined as the branching ratios of dimeric product ions obtained by two MS/MS experiments:

$$R_{\text{chiral}} = \frac{I_R/I_{\text{ref}(1)^*}}{I_S/I_{\text{ref}(2)^*}} \quad (3)$$

Being  $R_{\text{chiral}}$  a numerical value capable to indicate of the degree of chiral distinction under the employed analytical conditions, it can be manipulated by changing the  $M$  or the  $\text{ref}^*$ . Moreover, the farther  $R_{\text{chiral}}$  is from unity, the higher the degree of chiral recognition is obtained.  $R_{\text{chiral}}$  values equal to 1, indicate no chiral discrimination under the employed analytical conditions, which means that the  $M$  and  $\text{ref}^*$  ligand fails to create stereochemically dependent interactions with the enantiomers. Toward to increase the  $R_{\text{chiral}}$  value, different reference compounds or metals should be then tested (Tao et al., 2000).

A possible drawback of this method is the availability of both pure enantiomers to construct of the calibration curve. However, as previously mentioned, MS spectra from the  $M(\text{II})$ ,  $A$ , and  $\text{ref}^*$  mixtures are constituted by a series of signals with different  $A$ :  $\text{ref}^*$  stoichiometry (Figure 2). Taking advantage of this, Tao et al. (2002) developed a new method, the so-called quotient ratio method, for the evaluation the  $[M^{\text{II}}(A)_2(\text{ref}^*)-H]^+$  trimeric cluster ion, which contains two molecules of analyte and only one molecule of reference compound. When fragmented, this trimeric cluster ion allows the formation of  $[M^{\text{II}}(A)(\text{ref}^*)-H]^+$  and  $[M^{\text{II}}(A)_2-H]^+$  dimeric ions. Hence, for this competitive dissociation, the  $R$  value is proportional to the  $\Delta(\Delta G)$  of the  $\text{ref}^*$  instead to the analyte ( $A$ ). Consequently, by using two enantiomeric reference ( $\text{ref}^*_R$  and  $\text{ref}^*_S$ ), it is possible calculate the  $\Delta(\Delta G)$  for both  $[M^{\text{II}}(A)(\text{ref}^*_R)-H]^+$  and  $[M^{\text{II}}(A)(\text{ref}^*_S)-H]^+$  dimeric ions, as follows (Equation 4):

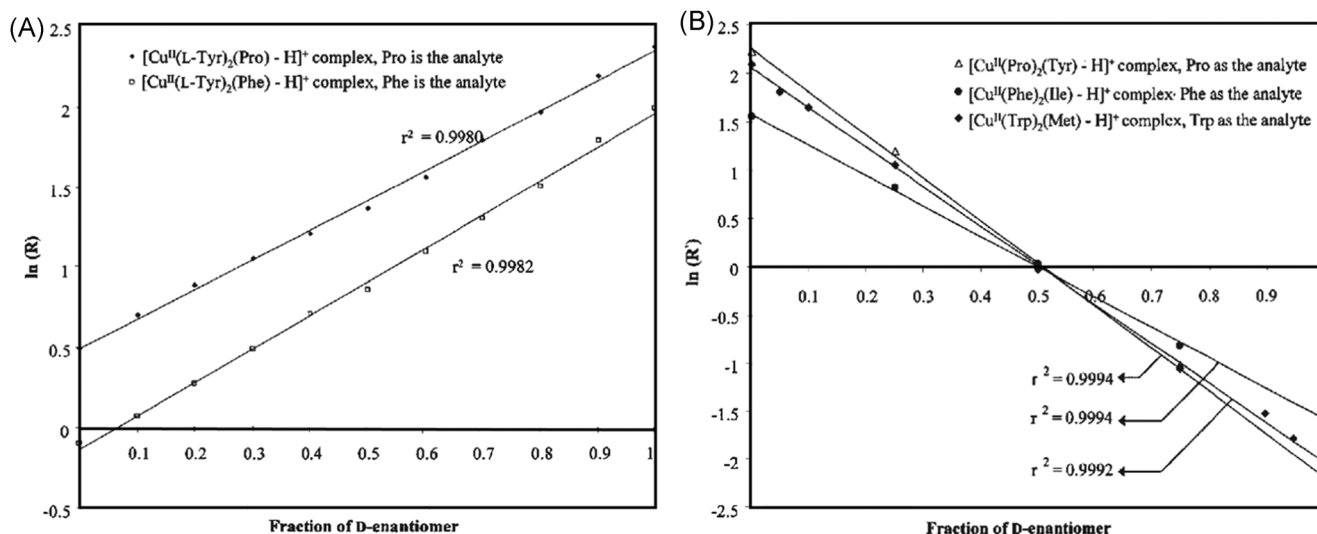


**FIGURE 4** (A) Calibration curves for chiral analysis of various amino acids using single-ratio method with the  $[Cu^{\text{II}}(A)(\text{ref}^*)_2-H]^+$  system. (B) Calibration curves for chiral analysis of various amino acids using the quotient-ratio method. Reproduced with permission from Tao et al. (2000)

$$RR = \frac{R_R}{R_S} = \frac{[M(A)(ref^*R) - H]^+ / [M(A)_2 - H]^+}{[M(A)(ref^*S) - H]^+ / [M(A)_2 - H]^+} \quad (4)$$

In this case, the differences in the abundances of  $[M^{II}(A)(ref^*_R) - H]^+$  and  $[M^{II}(A)(ref^*_S) - H]^+$  fragment ions represent the different energies required to generate them. Because of both diastereomeric forms are each measured relative to the abundance of  $[M^{II}(A)_2 - H]^+$  reference fragment ion in the same MS/MS spectrum, when Equation (4) is calculated, the obtained RR depends on the enantiomeric composition of the analyte (A). Again, a calibration curve can be obtained, in which every calibration point is the result of two consecutive measurements using optically pure  $ref^*_R$  and  $ref^*_S$  and the relative calculation of two RR (Figure 4B).

Lastly, a further evolution of the kinetic method for chiral analysis, which employs a fixed (i.e., non-dissociating) ligand as well as the usual A and  $ref^*$  ligands has been proposed (Wu & Cooks, 2003). In this variant, one of the two identical reference ligands has been replaced with  $L^{fixed}$ , an easily deprotonated compound with high metal affinity. Consequently, competitive fragmentations still occur, through the loss of the A and  $ref^*$  ligands, but the strongly chelated  $L^{fixed}$  will not be lost, as illustrated in Figure 5.

The advantages of this new method are the dissociation kinetics simplification and the chiral recognition optimization by changing the properties of the fixed ligand (e.g., size and functionality). Wu et al. proposed the chiral distinction of 4-benzyl-2-oxazolidinone by using the simplest chiral amino acid (alanine) as  $ref^*$  group and a series of glycine-alanine peptides of various sequences and increasing sizes as fixed ligands. Increasing the size of the fixed ligand forces the analyte and the reference ligand closer together, resulting in stronger metal-ligand and ligand-ligand interactions, and accordingly, this is expected to lead to improved chiral discrimination (Wu & Cooks, 2003).

Considering all the development introduced by the authors, the kinetic method proves to be a valid approach

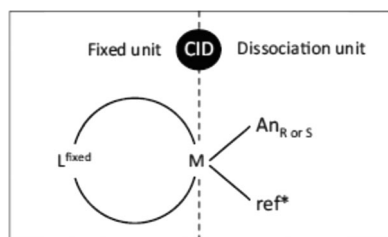


**FIGURE 5** Schematic diagram of the fixed-ligand kinetic method for chiral analysis. Reproduced with permission from Wu & Cooks (2003)

to obtain the characterization of racemic samples but his application may take considerable effort to identify appropriate reference ligands and metal ions suitable to obtain strong enantiomeric discrimination.

### 3 | DISTINCTION OF ISOMERIC/ISOBARIC COMPOUNDS IN A MIXTURE USING THE SY TECHNIQUE

The degree of parent ions survival in the collisional excitation process plotted against the employed excitation voltage is typically used in the energy resolved mass spectrometry experiments (ERMS). In these experiments, the SY parameter can be calculated during data elaboration, following the equation:

$$SY = \frac{I_M}{I_M + \sum I_F} \quad (5)$$

where,  $I_F$  represents the intensities of fragment ions and  $I_M$  represents the precursor ion intensity. SY values span from 1 (no precursor fragmentation, at collision energy = 0) to 0 (all precursor ions are fragmented, at high collision voltage values).

Generally, 10  $\mu$ M of analyte solution in water/methanol or water/acetonitrile mixtures is used to build its SY curve that (Figure 6) can be described by a sigmoid function. Each SY profile is characterized by the value of the collision energy in which the same intensities of precursor and product ions are obtained. This energy is defined as characteristic collision energy value (CCE)

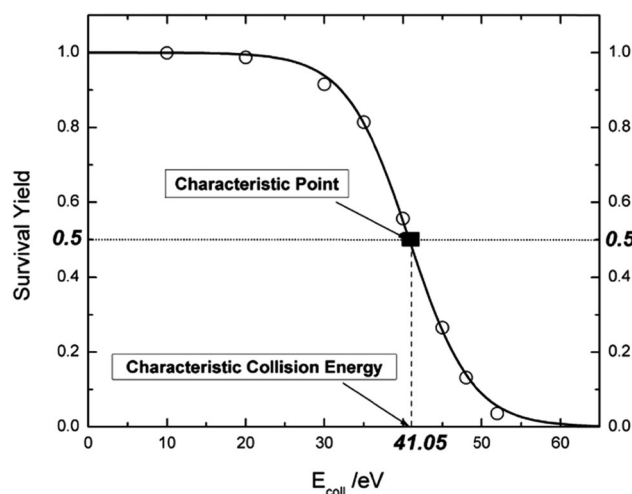


**FIGURE 6** Typical survival yield curve showing the CCE at SY = 0.5. Reproduced with permission from Memboeuf et al. (2010). CCE, characteristic collision energy

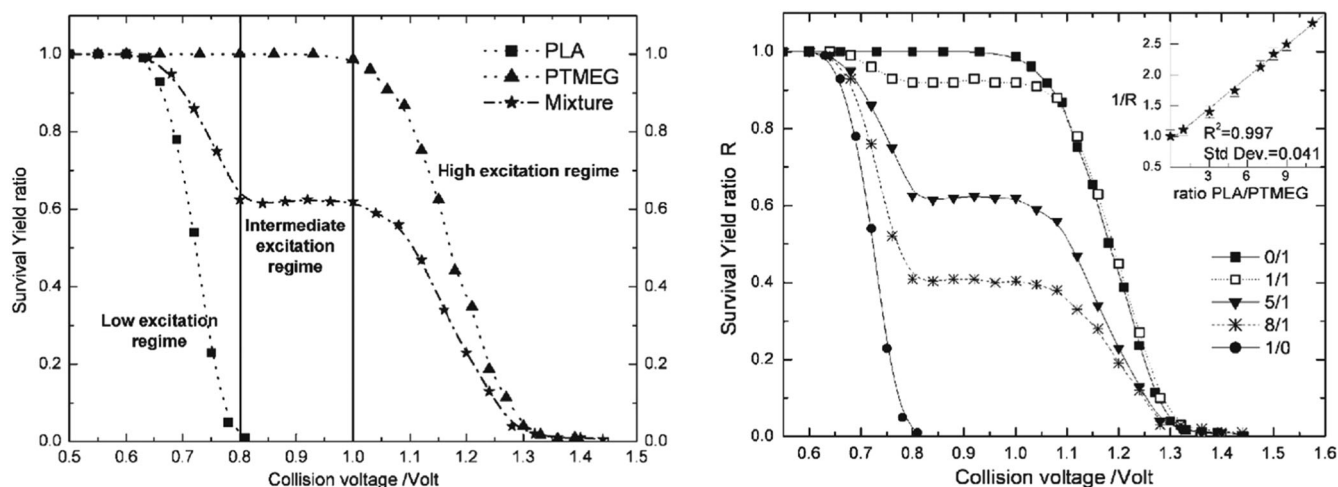


**FIGURE 7** (Left panel) Survival yield curves of pure compound 1 (filled squares with dotted line) and pure compound 2 (filled triangles with dotted line) and a 5:1 mixture of compound 1/compound 2 (filled stars with dot dashed line). The compound 1 and 2 are isobars, then they share the same precursor ion in ERMS experiments. (Right panel) SY curves for compounds 1 and 2 mixtures at different concentrations in the same experimental conditions. The inset shows the correlation between the inverse of the SY ratio at the plateau ( $R$ ) and the ratio between the compounds in mixture samples. Reproduced with permission from Memboeuf et al. (2011)

and corresponds to the supplied energy necessary to activate the dissociation channels allowing the “survival” of the 50 % of the precursor ions ( $SY = 0.5$ ).

The CCE (sometimes called CCV, in relation to the collision voltage applied) is structure-specific for each ion structure and represents the collision energy necessary to achieve a certain degree of fragmentation (Kertesz et al., 2009). The collision energy increases linearly with the molecular mass to a very good approximation and CCE is expected to increase similarly (Kuki et al., 2010; Memboeuf et al., 2010). For pure compounds, the typical SY curve shows a continuous and smooth decrease but without any plateau (Figure 6). On the contrary, the SY curve obtained by ERMS analysis of a mixture of two isobars having sufficiently different CCV values, a plateau is present, as displayed in Figure 7.

In the SY curve obtained for the 5:1 mixture of compound 1/compound 2 are reported in Figure 7 (left panel). Three regions have been evidenced: a “low excitation regime” for spectra acquired at excitation voltages  $<0.8$  V, an “intermediate excitation regime” for spectra acquired from 0.8 to 1 V (plateau), and a “high excitation regime” corresponding to the spectra acquired at excitation voltages  $>1$  V. The superimposition of SY curves from pure compounds 1 and 2 leads to highlights that at excitation voltages  $<0.8$  V (i.e., at low excitation regime) the SY of mixture is due to the sole fragmentation of the component 1 that, next to 0.8 V, is fully dissociated. At higher excitation voltages, the SY curve reach an intermediate excitation regime, which is guaranteed by the stability of the precursor ion of the

component 2 (that does not dissociate until the 1 V excitation voltage). Lastly, at excitation voltages  $>1$  V the SY curve decrease next to 0 due to the fragmentation channels of compound.

The SY approach does not limit to qualitative purposes and it can also be used for a quantitative analysis of its relative composition (Josse et al., 2015). Indeed, the SY curves obtained by analysis of the sample mixtures having different compound 1/compound 2 ratios, different profiles can be obtained (Figure 7, right panel). By increasing the amount of compound having lower CCV in the mixture (in this case, the compound 1), the shift of plateau toward lower SY ratio occurs. Being this trend proportional to compound 1 relative concentration, it is possible to obtain a linear function between the inverse of SY values ( $1/SY$ ) and the relative composition of the mixtures (insert in Figure 7, right panel).

Obviously, SY method well applies to the separation of isomers having sufficient difference in their CCV, so to give rise to the plateau. However, the SY method can be further implemented through the use of a “gas-phase collisional purification” (GPCP) (Dit Fouque et al., 2016). By introducing an additional mass-selection step ( $MS^3$ ) in the intermediate excitation regime, only the “survived” isomer (i.e., only precursor ion of compound having higher CCV) can be isolated and analyzed (Figure 8). Naturally, a multistage MS is then necessary to perform the GPCP strategy, which could be limited to tandem in time mass spectrometers (i.e., trapping-type instruments, IT) and would not be applicable to tandem in space

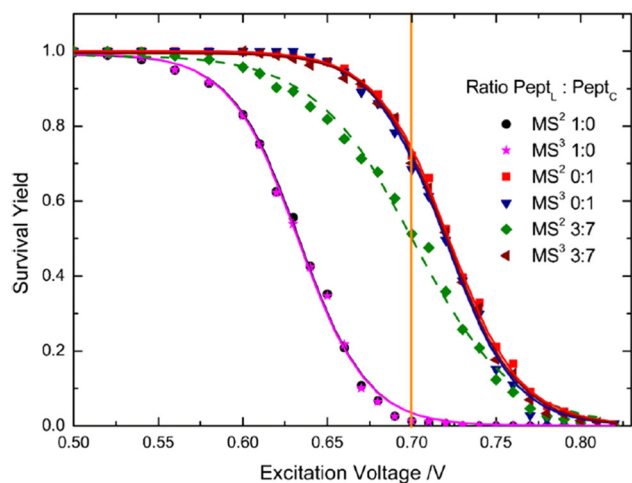


**FIGURE 8** SY curves for cesium-coordinated peptides with PeptL in MS<sup>2</sup> (circles) and in MS<sup>3</sup> (stars, after MS<sup>2</sup> at 0.62-V excitation voltage); PeptC in MS<sup>2</sup> (squares) and in MS<sup>3</sup> (down triangles, after MS<sup>2</sup> at 0.70-V excitation voltage); 3:7 mixture of PeptL/PeptC in MS<sup>2</sup> (diamonds) and, after “gas-phase collisional purification” in MS<sup>3</sup> (left triangles, after MS<sup>2</sup> at 0.70-V excitation voltage). Reproduced with permission from Dit Fouque et al. (2018). SY, survival yield [Color figure can be viewed at [wileyonlinelibrary.com](https://onlinelibrary.wiley.com)]

instruments (i.e., QqQ or QqToF). However, it is well known that ions fragmentation may be induced directly in the source before reaching the mass analyzer. Therefore, it is possible to expand the MS<sup>3</sup> capabilities of instruments not equipped with this functionality, such as QqQ or QqToF, by taking advantage of ESI in-source CID of the analyte (Dit Fouque et al., 2018; Maroto et al., 2020; Dit Fouque et al. 2021). The precursor ion isolated in the MS<sup>3</sup> stage at 0.70 V of excitation voltage (Figure 8, vertical line) undergoes to a second ERMS experiment and the obtained SY curve (Figure 8, left triangles) overlaps to that of pure compound. Pure peptide of obtained data is elaborated (Figure 8, squares).

Alternatively, it is possible to increase the CCV difference among all the isomers by isolating different precursors (i.e., cationized analyte ions instead of the protonated ones). This possibility is showed in Figure 9, in which are reported the SY curves obtained by ERMS analysis of isomer peptides mixtures obtained using the [M + K]<sup>+</sup> and [M + Cs]<sup>+</sup> as precursor ions. The differences between the CCV values of two pure peptides increase by switching from [M + H]<sup>+</sup> to [M + K]<sup>+</sup> or [M + Cs]<sup>+</sup> ions species.

Despite the improvement achieved by using different ionic adduct, the correct evaluation of SY values between the isomers can be compromised when the number of isomers increase ( $n > 3$ ) in the sample.

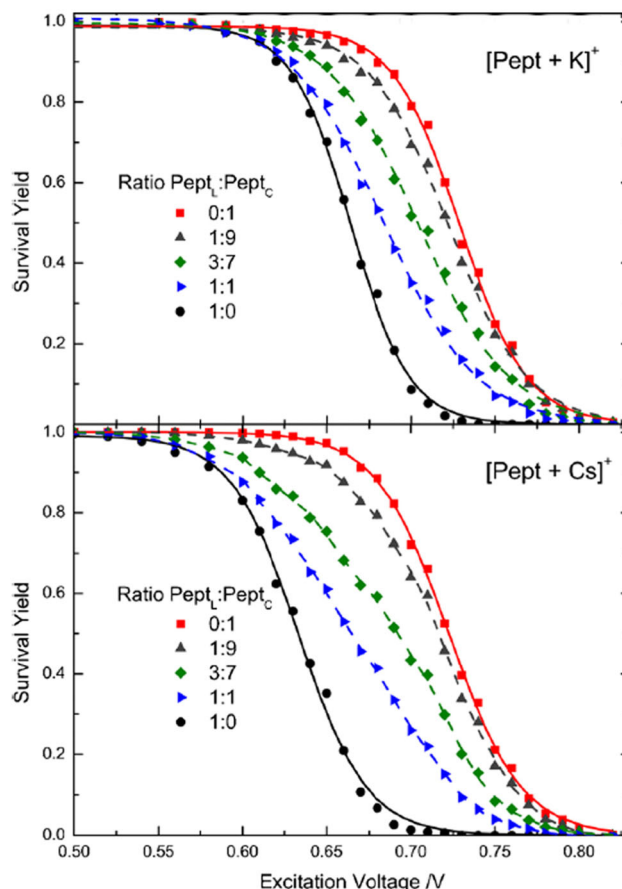


**FIGURE 9** SY curves for peptides mixtures of K<sup>+</sup>, and Cs<sup>+</sup> cationized precursor ions. Modified with permission from Dit Fouque et al. (2018). SY, survival yield [Color figure can be viewed at [wileyonlinelibrary.com](https://onlinelibrary.wiley.com)]

#### 4 | KINETICS OF THE ION-MOLECULE INTERACTION

The kinetic of the ion-molecule interactions has been investigated by to find out new ways to distinguish among isomers. The use of ion-molecule reactions without any exotic reagent or any chromatographic separation permits to obtain reliable data in a simple instrumental set-up and very quickly. In this application, the evaluation of the time of reaction between the isomers and the water present in the surround is primary; hence, only the ion trap MS system could be used.

Analytes cationization is known to occur under electrospray ionization (ESI). In presence of alkali or ammonium-containing solutions, it is possible to generate [M + cation]<sup>+</sup> ionic species, which have been shown to ameliorate sensitivity for molecules less prone to protonation. This is typically the case of carbohydrates, which form multidentate interactions with metal cations (Na<sup>+</sup>, Li<sup>+</sup>) thanks their poly-hydroxyl residues. Recently, water aduction kinetic and residual unreactive lithium-coordinated



carbohydrates has been used to distinguish the monosaccharides (pentoses or hexoses) and disaccharides isomers (Campbell, Chen, Glish, 2017; Campbell, Chen, Wallbillich, et al., 2017; Campbell et al., 2018). Indeed, once inside the quadrupole ion trap, part of these lithium-coordinated carbohydrates may add a water molecule, resulting in the new species  $[M + Li + H_2O]^+$  at 18 Da higher. This behavior can be explained by  $Li^+$  capability of binding up to six waters molecules in its first hydration shell (Rodgers & Armentrout, 1997). Consequently, when the parent ion  $[M + Li]^+$  is isolated into the quadrupole ion trap, “empty” sites where the lithium can still coordinate to one or two oxygens may remain reactive toward background water molecules. Because of carbohydrates tautomerisms (furanose or pyranose form), structure flexibility is restricted and the number of oxygens capable of coordinating to the lithium is limited. This makes some site unable to adduct water molecule and limits both the rate of water reaction and the final amount of unreactive (i.e.,  $[M + Li]^+$ ) fraction for each isomer. Hence, the ratio of  $[M + Li]^+ / ([M + Li]^+ + [M + Li + H_2O]^+)$  after all the reactive form has reacted, can be calculated and used to distinguish the isomers.

Each analyte 10  $\mu$ M solution was analyzed individually with addition of 100  $\mu$ M lithium acetate in 50/50 water/methanol and it is introduced by direct infusion ESI at a solvent flow rate of 2  $\mu$ L/min. To obtain data about the kinetics of water adduction reaction, increasing delay times (0, 10, 20, 30, 40, and 50 ms) were applied the isolated of  $[M + Li]^+$  species (i.e., between ion isolation and the subsequent mass analysis ejected ions out the ion trap).

Plotting the residual fraction of unreacted  $[M + Li]^+$  versus the applied delay time results in a clear exponential decay (Figure 10, left panel).

Because of some unreacted  $[M + Li]^+$ , decay curves have an asymptote and the corrected reaction rate ( $R_R$ ) at for each delay time can be calculated by the following equation:

$$R_R = \frac{(1 - R_U)(I_{[M+Li]^+} + I_{[M+Li+H_2O]^+}) - I_{[M+Li+H_2O]^+}}{(1 - R_U)(I_{[M+Li]^+} + I_{[M+Li+H_2O]^+})} \quad (6)$$

Therefore, plotting  $\ln(R_R)$  versus time yields a linear trend as expected (Figure 10, right panel). Author concluded that using both the unreactive fractions and the corrected reaction rates is possible to separate all the carbohydrates isomers. To evaluate the method reliability for quantitative purposes, a mixture of fructose and glucose at different ratios was analyzed. A linear calibration curve is obtained when reaction rate is plotted versus the percentage of fructose (Figure 11A). Alternatively, a calibration curve could be generated by plotting the unreactive fraction versus the fructose %. However, this will result in a fourth-order polynomial curve to interpolate data (Figure 11B), giving lower sensitivity at higher fructose % and poorer accuracy at lower fructose percentages. Three samples of high fructose corn syrup (HFCS) were analyzed: 45-HFCS, 52-HFCS, and 90-HFCS and obtained data revealed a fructose content 41.5 %, 57.1 %, and 86.7 %, respectively. The percent error associated to these measurements were 1.1 %, 3.9 %, and 3.6 %, thus demonstrating method accuracy (Campbell, Chen, Wallbillich, et al. 2017).

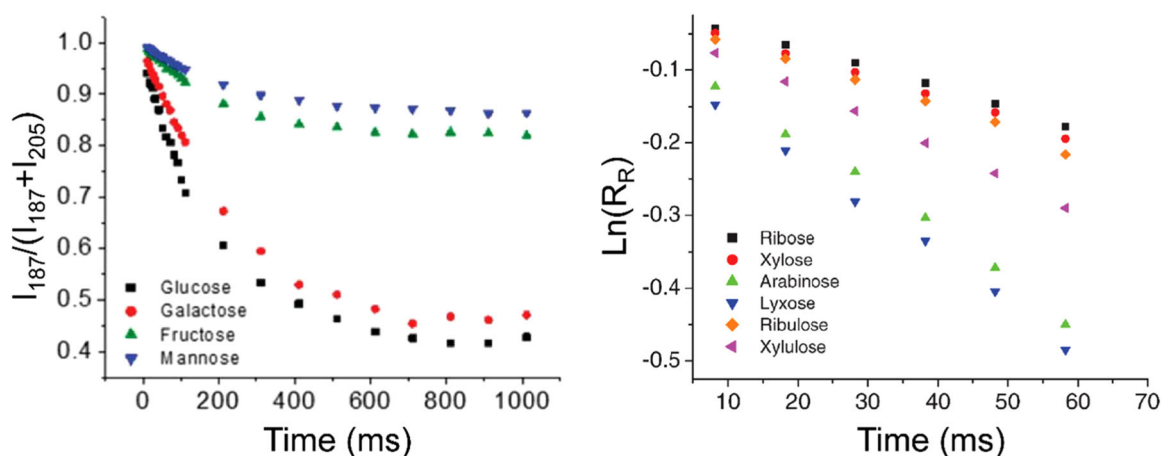


**FIGURE 10** (Left panel) Example of exponential decay of fraction of  $[M + Li]^+$  that has not yet reacted versus the delay time obtained from a series of hexoses. (Right panel) Example of natural logarithm of reaction rate of  $[M + Li]^+$  with water versus the delay time obtained from a series of pentoses. Reprinted with permission from Campbell, Chen, Glish (2017) and Campbell, Chen, Wallbillich, et al. (2017) [Color figure can be viewed at [wileyonlinelibrary.com](http://wileyonlinelibrary.com)]

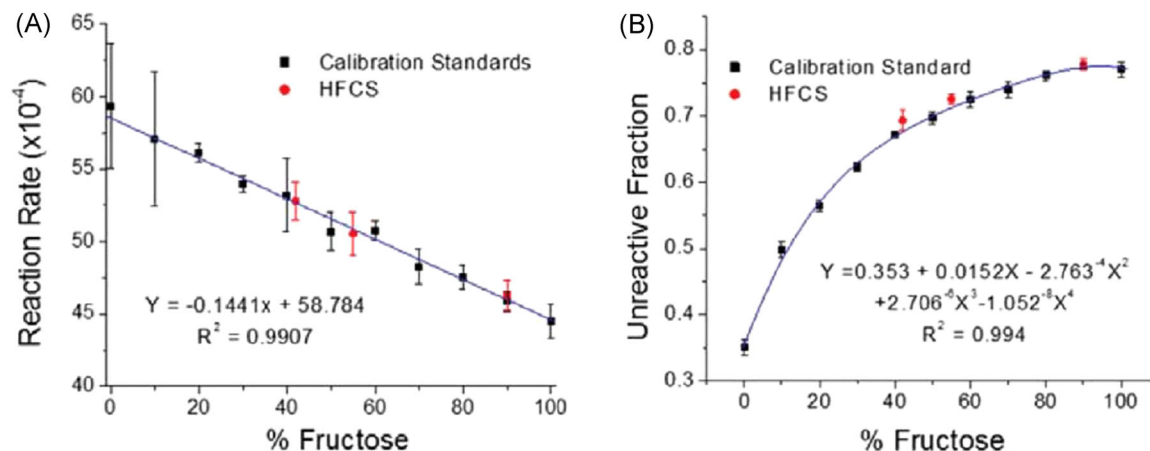
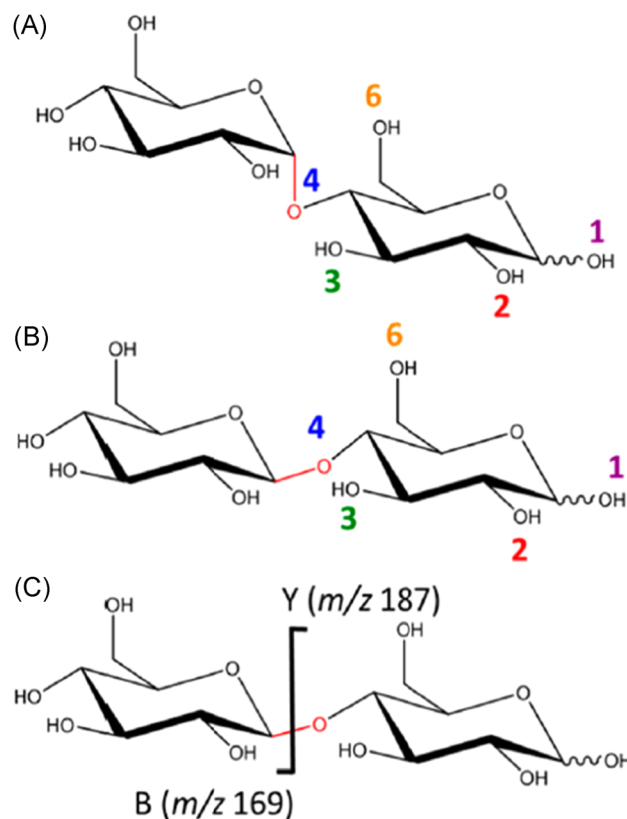


**FIGURE 11** Calibration curve for percent fructose as a function of (A) reaction rate and as a function of (B) unreactive fraction. Modified with permission from Campbell, Chen, Wallbillich, et al. (2017) [Color figure can be viewed at [wileyonlinelibrary.com](https://onlinelibrary.wiley.com/doi/10.1002/ms.21757)]

The kinetic method of water adduction is useful also for disaccharides identification, simply introducing a CID step to get the monosaccharidic form before the delay time (Campbell et al., 2018). The CID step at 0.85 V was applied to  $[M + Li]^+$  precursor ions and the product ions Y or B (at  $m/z$  187 and at  $m/z$  169, respectively) were then isolated, to apply the delay time scan. After cleavage of glycosidic bond, the lithium cation interacts with Y or B fragment ion, which in turns reacts with water yielding their peculiar unreactive fractions and reaction rates. By this method, three hetero-disaccharides (lactose, sucrose, and lactulose) can be distinguished. Moreover, authors demonstrated the possibility to distinguish both the linkage position and the anomeric conformation of ten Glucose–Glucose omo-disaccharides (Scheme 1).

As it can be seen in the left panel of Figure 12, the product ion Y (at  $m/z$  187) gave better separation for disaccharides having different linkage position, while the product ion B (at  $m/z$  169) gave better separation for determining anomeric configuration (right panel). The authors hypothesize that this behavior is due to the sites for lithium interaction in the product ions. Indeed, if in the B ion the lithium interacts with 2-hydroxyl, ring oxygen, and hydroxymethyl residues, in the Y ion the lithium will likely remain coordinated to oxygens involved in the glycosidic linkage. Method evaluation was applied to some samples naturally containing disaccharides. Beer, mushroom and vaping liquid of electronic cigarettes have been analyzed and the obtained results confirmed the ability of the method to identify the disaccharide isomer present in the samples.

Of note, if CID experiments of lithium cationized disaccharide were performed by a 1000 ms delay, without any prior isolation step, a signal at  $m/z$  205 along with the two at  $m/z$  169 and 187. This new peak was due to a water molecule adducted to Y ion species (previously



**SCHEME 1** Glucose–Glucose omo-disaccharide used as model for assessing the differences in the linkage position (at 1, 2, 3, 4, or 6) and in the anomeric configuration: (A) Alpha and (B) Beta. (C) Highlights the product ions obtained after CID experiments. Reproduced with permission from Campbell et al. (2018). CID, collision induced dissociation [Color figure can be viewed at [wileyonlinelibrary.com](https://onlinelibrary.wiley.com/doi/10.1002/ms.21757)]

detectable at  $m/z$  187), whilst actual peak at  $m/z$  187 consisted of both hydrated ions for B species (previously detectable at  $m/z$  169) and the unreactive Y ions at  $m/z$  187. Because the peak at  $m/z$  169 still represent

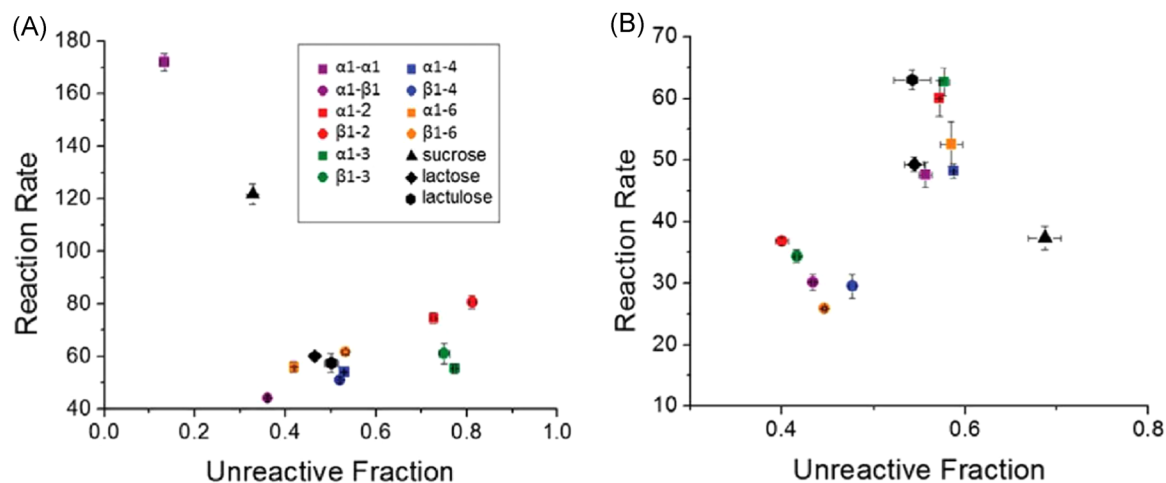


**FIGURE 12** Measured reaction rate versus unreactive fraction for each of the ten Glc–Glc omo-disaccharides and the three etero-disaccharides analyzed. Product ions at  $m/z$  187 (ion Y, left panel) and at  $m/z$  169 (ion B, right panel) obtained after CID experiments yield the two-dimensional separation of analytes. Reproduced with permission from Campbell et al. (2018). CID, collision induced dissociation [Color figure can be viewed at [wileyonlinelibrary.com](http://wileyonlinelibrary.com)]

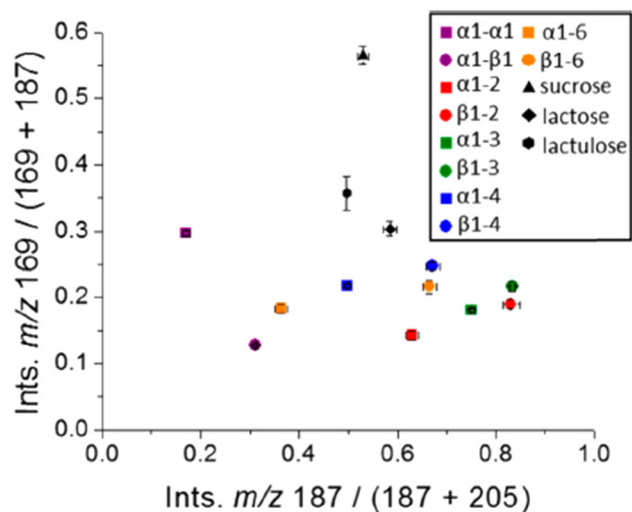


**FIGURE 13** Ratio of the signal intensity of ions at  $m/z$  169 to the sum of those at  $m/z$  169 and at  $m/z$  187 versus the ratio of the signal intensity of ions at  $m/z$  187 to the sum of those at  $m/z$  187 and at  $m/z$  205 after CID and 1000 ms of reaction time. Reproduced with permission from Campbell et al. (2018). CID, collision induced dissociation [Color figure can be viewed at [wileyonlinelibrary.com](http://wileyonlinelibrary.com)]

unreactive B species, the relative intensities among these ions permitted to distinguish analytes in a single experiment (Figure 13).

Of note, the evaluation of reaction rates for the ion–water reaction strongly depends on the internal energy of both ion and neutral reagent. Because of isomeric forms and internal energy are closely related, a distinction between the isomers is certainly possible. However, the recognition becomes decidedly more difficult when in the sample multiple isomers are present at once.

## 5 | POSTPROCESSING MATHEMATICAL ALGORITHM TO RESOLVE THE ISOMERS IN MS/MS SIGNAL

This approach is based on the assumption that a mixture of similarly fragmenting compounds will generate MS/MS spectra that are a combination of fragments from each component summed in proportions to their relative concentration, modeling approaches can be used (Kushnir et al., 2004). Then, the relative intensity of product ions and their branching ratios would be different among the isomers. The concentration of the isomers in unknown samples can be then calculated utilizing the ratio of the deconvoluted peak area to the area of the peak of an internal standard and the quantitative calibration.

The authors report that the algorithm is based on the following assumptions: (i) no peaks of the same mass transitions other than originating from the isomers are present under the target peak; (ii) the total acquired signal is a linear combination of signals from the co-eluting isomers; and (iii) the branching ratio of the monitored mass transitions is significantly different among the isomers. It is hardly that the first two assumptions can be satisfied in the analysis of unknown sample without the support of a chromatographic separation, because in presence of complex sample mixtures, the presence of interferences cannot to be excluded.

To overcome these difficulties, the linear equations deconvolution analysis (LEDA) is proposed (Menicatti et al., 2016a, 2016b, 2018, 2020). The LEDA algorithm is based on the same consideration reported above and the MS/MS data acquired by analysis of mixtures of isomers

in a postprocessing procedure are elaborated. This approach achieves a clear differentiation of the MS/MS signals coming from each isomer, by assigning their correct abundance in the sample without any chromatographic separation. However, by considering the tandem MS conditions, the components detected will have a common precursor ion, which can be related to the molecule ionic adduct or an isobaric interference fragment ion. In the latter case, the successive collisional dissociation leads to a pattern of different product ions that do not affect to the analyte signal. Different consideration should be made on the presence of two or more isomers in the sample that, beyond the same precursor ions, they share also the same product ions. Nevertheless, the same product ion formation from each isomer can be to occur with different intensity or different collision voltage. Therefore, by performing a series of ERMS experiments, it is possible to characterize the collision breakdown curves of each pure isomer, highlighting the different behavior.

The ERMS experiments consists of a series of product ion scan analyzes, monitoring the range from  $m/z$  50 to 650, and the collision energy is increased stepwise in the range 5–50 V. The 1  $\mu$ M analyte solution is infused, via syringe pump at 10  $\mu$ L/min; the protonated molecule was isolated and the abundances of product ions were monitored. The data obtained are used to construct the breakdown curves reported in Figure 14.

In Figure 14 are reported the breakdown curves obtained by elaboration of ERMS experiments carried out on two positional isomers (Menicatti et al., 2016b) by using a triple quadrupole with Argon as collision gas.

The precursor ion intensity (at  $m/z$  600) shows the same decreasing trend for both isomers. However, the curve and the composition of product ions are very different. The A isomer is characterized by only three evident product ions (at  $m/z$  205, 221, and 177), while the B isomer displays at least six product ions with different abundances distribution (listed in Figure 14). These breakdown curves highlight that precursor ion fragmentation, during CID process, is mediated by an isomerization step and lead to a characteristic product ions pattern for each isomer, allowing their distinction. Hence, the ERMS study on the pure isomers allows to emphasize their product ions differences which could be related both on the intensity of the signal or on the variation of the collision voltage abundances distribution. In this way, the MS/MS spectrum obtained by analysis of a mixture of isomers is a combination of the mass spectra of pure components added in proportions corresponding to their relative concentrations.

The aims of the mathematical approach present in the LEDA algorithm are to allow the deconvolution of the MS/MS spectrum, to recognize the components present in the sample and to evaluate their quantitative composition, avoiding the support of chromatographic separation.

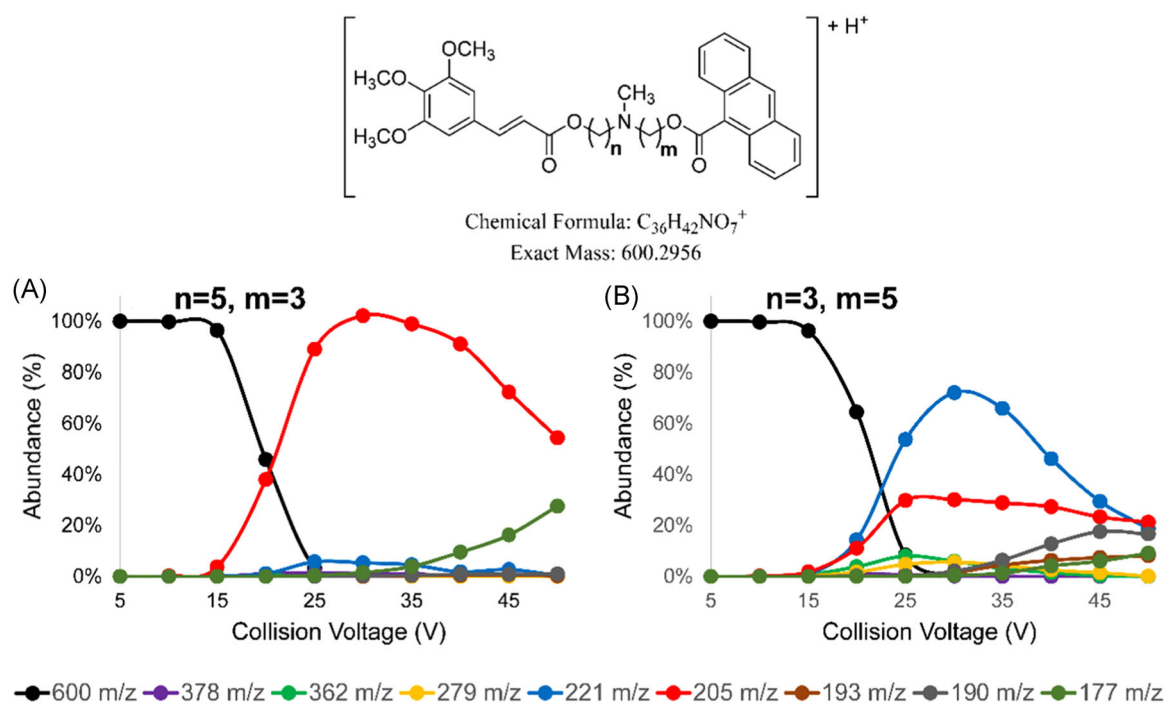


**FIGURE 14** The structures and breakdown curves of two positional isomers A and B. Reproduced with permissions from Menicatti et al. (2016b) [Color figure can be viewed at [wileyonlinelibrary.com](http://wileyonlinelibrary.com)]



To obtain reliable data, the relative abundances of the different product ions were calculated with respect to the reference ion abundance ( $R_i$ ), to avoid possible misleading results due to compound-dependent product ions yield. For this purpose, the  $R_i$  signal must be present in the same abundance in each isomer studied.

The authors in their applications proposed the available signal of the precursor ion, before its fragmentation, is acquired as  $R_i$ . Then, the abundance of precursor ion is obtained by analyzing the same concentration of each studied isomer in the identical MS/MS conditions. Therefore, the ratio between the abundance of each product ion ( $P_i$ ) acquired to  $R_i$  value, represents the yield of the product ion formation at the considered collision energy. To check the relationship between these ratios and the composition of isomer mixture, a series of standard solutions at different composition of the isomer pair is analyzed. By plotting the obtained intensity ratios from each mixture versus its theoretical composition, a linear correlation occurs that confirm the possibility of recognition of isomers by only elaboration of MS/MS data.

In Figure 15 are reported the regression lines for the most characteristic product ions (at  $m/z$  205 and 221) ratios of the tested positional isomers. Therefore, knowing the characteristic abundance ratios of the pure isomer, a deconvolution of these spectra is possible based on a series of linear regression equations as follows:

$$(P_i/R_i)_m = \sum_{x=1}^n (P_i/R_i)_x * [\%]_x \quad (7)$$

where  $(P_i/R_i)_m$  is the abundance ratio between the product ion ( $P_i$ ) and the reference ion ( $R_i$ ) measured ( $m$ ) in the sample;  $(P_i/R_i)_x$  are the characteristic abundance ratios between the product ion and the reference ion of

each pure isomer; and  $[\%]_x$  is the concentration (%) of each isomer in the sample.

In the binary mixture of isomers (A-B) a single equation related to the sole product ion ratio ( $P_i/R_i$ ) could be enough. Indeed, by assuming that only the isomer pair constitutes the MS/MS spectrum, the concentration of B is calculated as  $B \% = (1 - A) \%$ . However, in this case the possible contribution of signals from unknown isomers (or any interferent having the same product and reference ions) is neglected. Therefore, to avoid ill-conditioned algorithm, the resolution of the mixtures of  $n$  isomers is a matrix composed at least by  $n$  equations (Equation 7) is required (LEDA). In our case, the experimental data to be used are the abundance ratios of product/reference ions selected (MRM transitions) during MS/MS method set-up. Naturally, the mass transitions that showed significantly different among the isomers are preferably selected. In some cases, the analyte produces few product ions or their intensity is very low (i.e., isomer A in Figure 1); hence, to comply the number of equations requires by the LEDA algorithm, it can selected the same product ion but at different collision voltages. All calculations for the deconvolution MS/MS data are processed using an Excel™ macro. The recognition of isomers analysis is performed by applying the LEDA algorithm to the MS/MS signal intensities, allowing the relative amounts (%) of each component present in the sample. Then, to determine absolute concentrations of the constituents of a mixture, the resulted abundances of identified isomers are reported to corresponding calibration curve. Otherwise, when the sample is introduced in the mass spectrometer by flow injection analysis (FIA) or after a conventional chromatography separation, the LEDA can be applied to individual MS/MS data point. By this approach, each MRM signals are deconvoluted “scan-by-scan” and peak

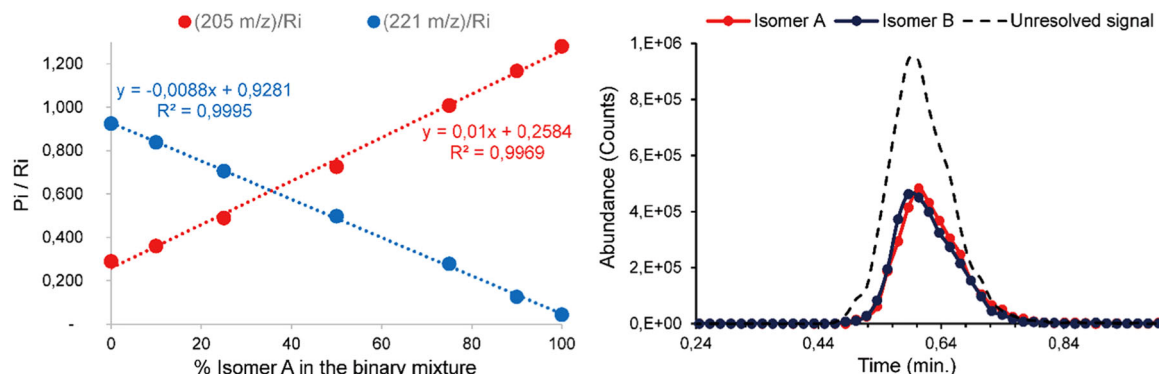


**FIGURE 15** The linear correlation between the intensity ratios of product ions (at  $m/z$  205 and 221) and  $R_i$  of the tested positional isomers versus nominal concentration of mixture (right panel). The MS/MS FIA signal of 1:1 mixture of 300 nM of isomers (black dotted line) and its deconvolution by LEDA matrix with isomer distinction (red line isomer A and blue line isomer B). Unpublished data, courtesy of Prof. G. Bartolucci [Color figure can be viewed at [wileyonlinelibrary.com](http://wileyonlinelibrary.com)]

integration would be performed on the deconvoluted data points. The deconvoluted peak intensities allow the determination of the relative amounts of the components in the sample. In Figure 2 is reported the MS/MS signal of FIA analysis of 1:1 mixture of 300 nM of isomer A and B (black dotted line) and its deconvolution by LEDA matrix with isomer distinction (red line isomer A and blue line isomer B).

To verify the LEDA reliability also in the conventional LC-MS/MS analysis, a series of plasma samples containing a mixture of unresolved isomers, are processed. In some cases, the authors observed that LEDA results gave a low signal purity of the isomer identified. However, the quantitative data, obtained by the abundances ratios between deconvoluted signal of quantitation ion and IS, were in accordance to the expected ones. Carefully examining those MRM signals, it was noted that these occurrences could be determined by Ri abnormal signals. The abundance of Ri signal could be affected by possible matrix interferences that may compromise the absolute value of the Pi/Ri ratios. However, this effect was distributed to all the product ions ratios employed to compile the LEDA algorithm; hence, the isomer assignment was not altered. Probably, the unassigned signal corresponds to the abundance of precursor ion coming from the matrix interferences (Menicatti et al., 2016a, 2018).

The LEDA ability to deconvolute raw MS/MS signals increases with the number of linear equations considered (i.e., in an over-determined matrix system). The resulted non-square matrix can be used when the value of the characteristic Pi/Ri ratios among the isomers are too close or high number of isomers ( $n > 2$ ) are present. In this case, the LEDA algorithm improves its efficiency and allows the correct partition of the MS/MS precursor ion signal for each isomer, which is used to estimate the ratio value with the abundance of IS (PAR) and finally to calculate its concentration by respective calibration curve (Menicatti et al., 2020).

## 6 | CONCLUSIONS

The features of tandem MS experiments applied in the recognition of isomers are presented and discussed in present review. The question to solve is whether it is possible to distinguish a mixture of isomers by using only the ion separation ability of MS/MS methods. Indeed, the use of tandem MS methods provide many advantages, among which the most important ones are the sensitivity, the reliability and the faster analysis.

MS is still commonly thought of as unable to distinguish isomers in mixture since as long as each

component gives a similar MS or MS/MS spectra under most traditional operative conditions. Moreover, several techniques reported in the literature appear to be compound-specific approaches, instead to proposing a standardizable one. Therefore, we have highlighted the key aspects that permit to discriminate between the isomers, allowing their separation. Relying on the tandem MS approach, fundamental steps to be explore are: the selection of precursor ion, its fragmentation through CID mechanism and its product ions analysis. The selection of most informative precursor ion allows achieving a high specificity in the characteristic product ions formation and their intensity. This occurs in the enantiomeric recognition by using the kinetic method proposed by Cooks' group. The formation of the trimeric cluster ion in gas phase, directly in ESI source, and its MS/MS analysis permits a sensitive, simple a quickly enantiomers separation. Alternatively, the CID energetic study (i.e., ERMS experiments) permits the separation isobar components by plotting their SY curve. Indeed, the SY profile allows detecting if the sample is pure or composed of more components with the same precursor ion. Naturally, each component of the mixture must have a significant difference of CCE (or CCV) value, to make this separation effective. Then, it can be introduced a further isolation step ( $MS^3$ ), carried out on the "survived" precursor ion, by performing a GPCP Taking the advantage to the ion trap features, Glush et al. proposed to maintain the lithium-coordinated precursor ion for a certain time (named "delay time") to allow his reaction with the surrounding water. However, also in this application, it is very important the selection of an active precursor ion toward the water adduct formation. The selective signals capable to distinguish the isomers are the precursor ion ( $[M + Li]^+$ ) and its water adduct ( $[M + Li + H_2O]^+$ ), whose relative intensities are used to calculate the unreactive fraction ( $R_U$ ) and corrected reaction rate ( $R_R$ ) values characteristic for each isomer studied.

Finally, a mathematical approach (LEDA algorithm) for the deconvolution of an isomer mixture MS/MS signal has been recently proposed by Menicatti et al. LEDA algorithm uses the product ions intensities obtained by a FIA to separate the isomers present in the sample, allowing both quali- and quantitative evaluations. To obtain reliable results, ERMS study on each isomer studied is needed to establish their breakdown curves and to select the most informative product ions at the characteristic collision voltage value. Despite its novelty, reported results are promising for the extensive application of LEDA approach to the isomers analysis without any chromatographic separation.

## ACKNOWLEDGMENT

Open Access Funding provided by Università degli Studi di Firenze within the CRUI-CARE Agreement.

## REFERENCES

- Augusti, D. V., R. Augusti, F. Carazza and R. G. Cooks (2002a). "Quantitative determination of the enantiomeric composition of thalidomide solutions by electrospray ionization tandem mass spectrometry." *Chemical Communications* 19: 2242-2243.
- Augusti, D. V., F. Carazza, R. Augusti, W. A. Tao and R. G. Cooks (2002b). "Quantitative chiral analysis of sugars by electrospray ionization tandem mass spectrometry using modified amino acids as chiral reference compounds." *Analytical Chemistry* 74(14): 3458-3462.
- Augusti, D. V. and R. Augusti (2005). "Determination of the enantiomeric composition of ibuprofen solutions via a rapid and sensitive mass spectrometry method." *Tetrahedron: Asymmetry* 16(10): 1881-1885.
- Awad, H. and A. El-Aneel (2013). "Enantioselectivity of mass spectrometry: Challenges and promises." *Mass Spectrometry Reviews* 32(6): 466-483.
- Basso, E., A. Chilin, A. Guiotto and P. Traldi (2003). "Electrospray mass spectrometry in the differentiation of some isomeric trimethylfurocoumarins." *Rapid Communications in Mass Spectrometry* 17(24): 2781-2787.
- Berthod, A. (2010). Ch.1 Chiral recognition mechanisms in enantiomers separations: A general view. Chiral recognition in separation methods. A. Berthod (Ed.), Springer-Verlag, Berlin, Heidelberg.
- Cabrele, C., T. A. Martinek, O. Reiser and Ł. Berlicki (2014). "Peptides containing  $\beta$ -amino acid patterns: Challenges and successes in medicinal chemistry." *Journal of Medicinal Chemistry* 57(23): 9718-9739.
- Campbell, M. T., D. Chen and G. L. Glish (2017). "Identifying the D-pentoses using water adduction to lithium cationized molecule." *Journal of the American Society for Mass Spectrometry* 28(7): 1420-1424.
- Campbell, M. T., D. Chen, N. J. Wallbillich and G. L. Glish (2017). "Distinguishing biologically relevant hexoses by water adduction to the lithium-cationized molecule." *Analytical Chemistry* 89(19): 10504-10510.
- Campbell, M. T., D. Chen and G. L. Glish (2018). "Distinguishing linkage position and anomeric configuration of glucose-glucose disaccharides by water adduction to lithiated molecules." *Analytical Chemistry* 90(3): 2048-2054.
- Chen, J., C.-J. Zhu, Y. Chen and Y.-F. Zhao (2002). "Enantiomeric quantification of the bioactive peptide seryl-histidine methyl ester by electrospray ionization mass spectrometry and the kinetic method." *Rapid Communications in Mass Spectrometry* 16(12): 1251-1253.
- Chouinard, C. D., C. R. Beekman, R. H. J. Kemperman, H. M. King and R. A. Yost (2017). "Ion mobility-mass spectrometry separation of steroid structural isomers and epimers." *International Journal for Ion Mobility Spectrometry* 20(1): 31-39.
- Clowers, B. H., P. Dwivedi, W. E. Steiner, H. H. Hill and B. Bendiak (2005). "Separation of sodiated isobaric disaccharides and trisaccharides using electrospray ionization-atmospheric pressure ion mobility-time of flight mass spectrometry." *Journal of the American Society for Mass Spectrometry* 16(5): 660-669.
- Cooks, R., J. S. Patrick, T. Kotiaho and S. A. McLuckey (1994). "Thermochemical determinations by the kinetic method." *Mass Spectrometry Reviews* 13(4): 287-339.
- Cooks, R. G. and P. S. H. Wong (1998). "Kinetic method of making thermochemical determinations: Advances and applications." *Accounts of Chemical Research* 31(7): 379-386.
- Creese, A. J., J. Smart and H. J. Cooper (2013). "Large-scale analysis of peptide sequence variants: The case for high-field asymmetric waveform ion mobility spectrometry." *Analytical Chemistry* 85(10): 4836-4843.
- Drazic, A., L. M. Myklebust, R. Ree and T. Arnesen (2016). "The world of protein acetylation." *Biochim Biophys Acta* 1864(10): 1372-1401.
- Huang, L., Z. Gao, X. Yin, Q. He and Y. Pan (2020). "Exploration of disaccharide as reference towards chiral recognition by the kinetic method." *Rapid Communications in Mass Spectrometry* 34(10): e8764.
- Hurtado, P. P. and P. B. O'Connor (2012). "Differentiation of isomeric amino acid residues in proteins and peptides using mass spectrometry." *Mass Spectrometry Reviews* 31(6): 609-625.
- Dit Fouque J D., A. Maroto and A. Memboeuf (2016). "Purification and quantification of an isomeric compound in a mixture by collisional excitation in multistage mass spectrometry experiments." *Analytical Chemistry* 88(22): 10821-10825.
- Dit Fouque J D., R. Lartia, A. Maroto and A. Memboeuf (2018). "Quantification of intramolecular click chemistry modified synthetic peptide isomers in mixtures using tandem mass spectrometry and the survival yield technique." *Analytical and Bioanalytical Chemistry* 410(23): 5765-5777.
- Dit Fouque J D., A. Maroto and A. Memboeuf (2021). "Structural analysis of a compound despite the presence of an isobaric interference by using in-source collision induced dissociation and tandem mass spectrometry." *Journal of Mass Spectrometry* 56(2) e4698.
- Josse, T., J. De Winter, P. Dubois, O. Coulembier, P. Gerbaux and A. Memboeuf (2015). "A tandem mass spectrometry-based method to assess the architectural purity of synthetic polymers: a case of a cyclic polylactide obtained by click chemistry." *Polymer Chemistry* 6(1): 64-69.
- Karthikraj, R., R. K. Chitumalla, K. Bhanuprakash, S. Prabhakar and M. Vairamani (2014). "Enantiomeric differentiation of  $\beta$ -amino alcohols under electrospray ionization mass spectrometric conditions." *Journal of Mass Spectrometry* 49(1): 108-116.
- Kertesz, T. M., L. H. Hall, D. W. Hill and D. F. Grant (2009). "CE50: Quantifying collision induced dissociation energy for small molecule characterization and identification." *Journal of the American Society for Mass Spectrometry* 20(9): 1759-1767.
- Kuki, A., L. Nagy, A. Memboeuf, L. Drahos, K. Vekey, M. Zsuga and S. Keki (2010). "Energy-dependent collision-induced dissociation of lithiated polytetrahydrofuran: effect of the size on the fragmentation properties." *Journal of the American Society for Mass Spectrometry* 21(10): 1753-1761.
- Kumari, S., S. Prabhakar and M. Vairamani (2008). "Halogen-substituted phenylalanines as enantioselective selectors for enantioselective discrimination of amino acids: effect of halogen." *Rapid Communications in Mass Spectrometry* 22(9): 1393-1398.

- Kushnir, M. M., A. L. Rockwood and G. J. Nelson (2004). "Simultaneous quantitative analysis of isobars by tandem mass spectrometry from unresolved chromatographic peaks." *Journal of Mass Spectrometry* 39(5): 532-540.
- Lambeth, T. R., D. L. Riggs, L. E. Talbert, J. Tang, E. Coburn, A. S. Kang, J. Noll, C. Augello, B. D. Ford and R. R. Julian (2019). "Spontaneous isomerization of long-lived proteins provides a molecular mechanism for the lysosomal failure observed in Alzheimer's disease." *ACS Central Science* 5(8): 1387-1395.
- Laphorn, C., F. Pullen and B. Z. Chowdhry (2013). "Ion mobility spectrometry-mass spectrometry (IMS-MS) of small molecules: Separating and assigning structures to ions." *Mass Spectrometry Reviews* 32(1): 43-71.
- Lee, M.-K., A. P. Kumar and Y.-I. Lee (2008). "Kinetic method for enantiomeric determination of thyroid hormone (d,l-thyroxine) using electrospray ionization tandem mass spectrometry (ESI-MS/MS)." *International Journal of Mass Spectrometry* 272(2): 180-186.
- Lehmann, W. D., A. Schlosser, G. Erben, R. Pipkorn, D. Bossemeyer and V. Kinzel (2000). "Analysis of isoaspartate in peptides by electrospray tandem mass spectrometry." *Protein Science* 9(11): 2260-2268.
- Maroto, A., D. Jeanne Dit Fouque and A. Memboeuf (2020). "Ion trap MS using high trapping gas pressure enables unequivocal structural analysis of three isobaric compounds in a mixture by using energy-resolved mass spectrometry and the survival yield technique." *Journal of Mass Spectrometry* 55(7): e4478.
- Memboeuf, A., A. Nasioudis, S. Indelicato, F. Pollreis, Á. Kuki, S. Kéki, O. F. van den Brink, K. Vékey and L. Drahoš (2010). "Size effect on fragmentation in tandem mass spectrometry." *Analytical Chemistry* 82(6): 2294-2302.
- Memboeuf, A., L. Jullien, R. Lartia, B. Brasme and Y. Gimbert (2011). "Tandem mass spectrometric analysis of a mixture of isobars using the survival yield technique." *Journal of the American Society for Mass Spectrometry* 22(10): 1744-1752.
- Menicatti, M., L. Guandalini, S. Dei, E. Floriddia, E. Teodori, P. Traldi and G. Bartolucci (2016a). "Energy resolved tandem mass spectrometry experiments for resolution of isobaric compounds: A case of cis/trans isomerism." *European Journal of Mass Spectrometry* 22(5): 235-243.
- Menicatti, M., L. Guandalini, S. Dei, E. Floriddia, E. Teodori, P. Traldi and G. Bartolucci (2016b). "The power of energy-resolved tandem mass spectrometry experiments for resolution of isomers: the case of drug plasma stability investigation of multidrug resistance inhibitors." *Rapid Communications in Mass Spectrometry* 30(3): 423-432.
- Menicatti, M., M. Pallecchi, S. Bua, D. Vullo, L. Di Cesare Mannelli, C. Ghelardini, F. Carta, C. T. Supuran and G. Bartolucci (2018). "Resolution of co-eluting isomers of anti-inflammatory drugs conjugated to carbonic anhydrase inhibitors from plasma in liquid chromatography by energy-resolved tandem mass spectrometry." *Journal of Enzyme Inhibition and Medicinal Chemistry* 33(1): 671-679.
- Menicatti, M., M. Pallecchi, M. Ricciutelli, R. Galarini, S. Moretti, G. Sagratini, S. Vittori, S. Lucarini, G. Caprioli and G. Bartolucci (2020). "Determination of coeluted isomers in wine samples by application of MS/MS deconvolution analysis." *Journal of Mass Spectrometry* 55(11): e4607.
- Ming, L., L. Zhiqiang, C. Huanwen, L. Shuying and J. Qinhan (2005). "Chiral quantification of D-, L-phenylglycine mixture using mass spectrometric kinetic method." *Journal of Mass Spectrometry* 40(8): 1072-1075.
- Nunez, A., Y. Sapozhnikova and S. J. Lehotay (2018). "Characterization of MS/MS product ions for the differentiation of structurally isomeric pesticides by high-resolution mass spectrometry." *Toxics* 6(4): 59.
- Pesavento, J. J., C. A. Mizzen and N. L. Kelleher (2006). "Quantitative analysis of modified proteins and their positional isomers by tandem mass spectrometry: Human histone H4." *Analytical Chemistry* 78(13): 4271-4280.
- Pittenauer, E. and G. Allmaier (2009). "The renaissance of high-energy CID for structural elucidation of complex lipids: MALDI-TOF/RTOF-MS of alkali cationized triacylglycerols." *Journal of the American Society for Mass Spectrometry* 20(6): 1037-1047.
- Posocco, B., M. Buzzo, L. Giodini, S. Crotti, S. D'Aronco, P. Traldi, M. Agostini, E. Marangon and G. Toffoli (2018). "Analytical aspects of sunitinib and its geometric isomerism towards therapeutic drug monitoring in clinical routine." *Journal of Pharmaceutical and Biomedical Analysis* 160: 360-367.
- Ramesh, M., B. Raju, R. Srinivas, V. V. Sureshbabu, T. M. Vishwanatha and H. P. Hemantha (2011). "Characterization of Nalpha-Fmoc-protected dipeptide isomers by electrospray ionization tandem mass spectrometry (ESI-MS(n)): effect of protecting group on fragmentation of dipeptides." *Rapid Communications in Mass Spectrometry* 25(14): 1949-1958.
- Rodgers, M. T. and P. B. Armentrout (1997). "Collision-induced dissociation measurements on Li+(H<sub>2</sub>O)<sub>n</sub>, n = 1-6: The first direct measurement of the Li+-OH<sub>2</sub> bond energy." *The Journal of Physical Chemistry A* 101(7): 1238-1249.
- Sawada, M., Y. Takai, H. Yamada, J. Nishida, T. Kaneda, R. Arakawa, M. Okamoto, K. Hirose, T. Tanaka and K. Naemura (1998). "Chiral amino acid recognition detected by electrospray ionization (ESI) and fast atom bombardment (FAB) mass spectrometry (MS) coupled with the enantiomer-labelled (EL) guest method." *Journal of the Chemical Society, Perkin Transactions 2*(3): 701-710.
- Scrivens, J. H., A. T. Jackson, K. R. Jennings, R. C. K. Jennings and N. J. Everall (2003). "High energy collision-induced dissociation (CID) product ion spectra of isomeric polyhydroxy sugars." *International Journal of Mass Spectrometry* 230(2): 201-208.
- Subramaniam, R., A. Östin, Y. Nygren, L. Juhlin, C. Nilsson and C. Åstot (2011). "An isomer-specific high-energy collision-induced dissociation MS/MS database for forensic applications: a proof-of-concept on chemical warfare agent markers." *Journal of Mass Spectrometry* 46(9): 917-924.
- Tao, W. A., D. Zhang, E. N. Nikolaev and R. G. Cooks (2000). "Copper (II)-assisted enantiomeric analysis of d,l-amino acids using the kinetic method: Chiral recognition and quantification in the gas phase." *Journal of the American Chemical Society* 122(43): 10598-10609.
- Tao, W. A. and R. G. Cooks (2001). "Parallel reactions for enantiomeric quantification of peptides by mass spectrometry." *Angewandte Chemie International Edition* 40(4): 757-760.
- Tao, W. A., F. C. Gozzo and R. G. Cooks (2001). "Mass spectrometric quantitation of chiral drugs by the kinetic method." *Analytical Chemistry* 73(8): 1692-1698.
- Tao, W. A., L. Wu, R. G. Cooks, F. Wang, J. A. Begley and B. Lampert (2001). "Rapid enantiomeric quantification of



- an antiviral nucleoside agent (D,L-FMAU, 2'-fluoro-5-methyl-beta,D,L-arabinofurano-syluracil) by mass spectrometry." *Journal of Medicinal Chemistry* 44(22): 3541-3544.
- Tao, W. A., R. L. Clark and R. G. Cooks (2002). "Quotient ratio method for quantitative enantiomeric determination by mass spectrometry." *Analytical Chemistry* 74(15): 3783-3789.
- Tao, W. A. and R. G. Cooks (2003). "Chiral analysis by MS." *Analytical Chemistry* 75(1): 25A-31A.
- Wang, B., J. Z. Shang, Y. J. Qin, B. N. Yan and X. H. Guo (2011). "Differentiation of alpha- or beta-aspartic isomers in the heptapeptides by the fragments of  $[M + Na]^+$  using ion trap tandem mass spectrometry." *Journal of the American Society for Mass Spectrometry* 22(8): 1453-1462.
- Wu, L., W. A. Tao and R. G. Cooks (2002). "Ligand and metal-ion effects in metal-ion clusters used for chiral analysis of alpha-hydroxy acids by the kinetic method." *Analytical and Bioanalytical Chemistry* 373: 618-627.
- Wu, L. and R. G. Cooks (2003). "Chiral analysis using the kinetic method with optimized fixed ligands: Applications to some antibiotics." *Analytical Chemistry* 75(3): 678-684.
- Wu, L. and R. G. Cooks (2005). "Chiral and isomeric analysis by electrospray ionization and sonic spray ionization using the fixed-ligand kinetic method." *European Journal of Mass Spectrometry* 11(2): 231-242.
- Wu, L., F. G. Vogt and D. Q. Liu (2013). "Flow-injection MS/MS for gas-phase chiral recognition and enantiomeric quantitation of a novel boron-containing antibiotic (GSK2251052A) by the mass spectrometric kinetic method." *Analytical Chemistry* 85(10): 4869-4874.
- Wu, Q., J.-Y. Wang, D.-Q. Han and Z.-P. Yao (2020). "Recent advances in differentiation of isomers by ion mobility mass spectrometry." *Trends in Analytical Chemistry* 124: 115801.
- Yol, A. M. and C. Wesdemiotis (2014). "Multidimensional mass spectrometry methods for the structural characterization of cyclic polymers." *Reactive and Functional Polymers* 80: 95-108.
- Zhang, D., W. A. Tao and R. G. Cooks (2001). "Chiral resolution of d- and l-amino acids by tandem mass spectrometry of Ni(II)-bound trimeric complexes." *International Journal of Mass Spectrometry* 204(1): 159-169.

**How to cite this article:** Crotti S, Menicatti M, Pallecchi M, Bartolucci G. Tandem mass spectrometry approaches for recognition of isomeric compounds mixtures. *Mass Spec Rev.* 2023;42:1244-1260.  
<https://doi.org/10.1002/mas.21757>